Industrial High Pressure Ethylene Polymerization Initiated By Peroxide Mixtures: A Reduced Mathematical Model For Parameter Adjustment

M. ASTEASUAIN, S. PEREDA, M. H. LACUNZA, P. E. UGRIN, *and* A. BRANDOLIN*

Planta Piloto de Ingeniería Química—UNS-CONICET
Camino la Carrindanga, km7–8000 Bahía Blanca–Argentina

We present a method for the adjustment of parameters in the mathematical modeling of industrial tubular reactors for high pressure polymerization of ethylene. We propose a reduced mathematical model for these reactors that aids in the task of model parameter update commonly done periodically in industrial plants. This reduced model was built from a detailed model for multiple peroxide and oxygen initiator systems we had developed before. Some of the assumptions in that rigorous model were reviewed in order to minimize computational effort. Good and faster predictions were obtained by assuming different constant jacket temperatures and pressures at each zone. Pressure pulse equations had to be included in the model. A simplification of the adjustment procedure is also proposed here. It consists in using only the reactions considered crucial for the description of this polymerization. The peroxide initiator and solvent mixtures were treated as fictitious unique initiator and solvent respectively. A procedure was established for the quick estimation of the kinetic parameters that represent initiator and solvent mixtures of different compositions. This resulted in a model that can be adjusted rapidly to predict the behavior of a specific industrial reactor. The reduced model was validated using experimental runs initiated by oxygen either alone or together with peroxide mixtures.

INTRODUCTION

The high pressure polymerization of ethylene in tubular reactors to produce branched low density polyethylene is a widely employed industrial process. It is carried out under rigorous operating conditions. For example, pressure ranges from 1300 to 3000 atm while temperature rises from 50°C to 330°C due to the exothermic polymerization. Moreover, a let-down valve located at the reactor exit is periodically opened to produce a pressure pulse which sweeps out the polymer from the walls (1, 2). Heat exchange in these reactors is controlled by several heating/cooling jackets, where water or vapor at different thermal levels flows under counter/current flow.

Reactor productivity and the molecular properties of the product are controlled by multiple injection of initiator mixtures, by monomer feedings at different locations along the reactor and by adding mixtures of low molecular weight chain transfer agents. The use of a mathematical model of the process is obviously a preferable design or predictive tool, in comparison with trial-and-error experiments at pilot or industrial scale.

The mathematical modeling of this process is not an easy task. The more rigorous the modeling is, the more accurate the predictions are expected to be. Nevertheless, in view of the computational cost, some simplifying assumptions are allowed, provided the loss of accuracy is not significant. So, an analysis of the incidence of model hypotheses on model results is worthwhile.

Once a model for the process has been developed, the next step is to adjust its predictions to plant data. This is done by proper manipulation of the model parameter values, mainly of those related to kinetic constants and equations containing heat transfer coefficients. Reviews of published kinetic parameters (1, 3, 4) demonstrated that the kinetic parameters available from the literature are rarely comparable. Kiparissides

*Corresponding author.

et al. (5) pointed out that one of the major problems in simulating LDPE industrial reactors is the selection of proper values for the kinetic parameters. Evidently, the simplifying assumptions, the process uncertainties and the specific features of a given reactor have a great influence on the final parameter values. It is also known that the range of experimental conditions available from an industrial reactor as data to carry out the model adjustment procedure is limited exclusively to values associated to the production of commercially valuable polyethylene only. A given set of kinetic parameters will be useful so long as the range of operating conditions for which it was determined is maintained, being of little predictive value when the operating conditions change significantly. In the latter case, a new adjustment will be required to preserve the predictive capability of the model. Lorenzini *et al.* (4) pointed out the great importance of easy tuning of kinetic parameters under changes in operating conditions for industrial applications. Moreover, when buying general purpose commercial software containing polymerization models, different parameter adjustments must be done for each particular reactor, this being more costly than the software itself.

A revision of previous experience on mathematical modeling (2) shows only few works that deal with some kind of parameter adjustment using industrial experimental data. Most of the published models (6–9) took their constants from previous literature reports, some of them obtained in laboratory experiments, instead. Those papers did not present any comparisons with experimental data. Goto *et al.* (10) and Lorenzini *et al.* (4) determined the kinetic parameters of their model from experimental data obtained in autoclave bench scale reactors. Other authors (4, 11, 12) did so through an analysis of experimental data from an industrial reactor. To perform the parameter estimation Zabisky *et al.* (2) also used data from the literature. We previously reported (1, 13) two-step and three-step parameter optimizations using data from two industrial reactors. The parameters controlling temperature were optimized first and afterwards, those influencing molecular structure were considered.

Most of the existing works studied a unique injection of a single initiator, either peroxide or oxygen. Zabisky *et al.* (2) considered monomer-initiator multiple injections, but they did not disclose values of the kinetic parameters due to proprietary issues. We also incorporated multiple injection of peroxide mixtures together with oxygen (1), for a situation that was typical of those in the local industry. Our kinetic parameters were in the range of those already reported in the open literature.

In most cases, a lack of detailed explanations on the adjustment procedure itself was observed. Villermaux *et al.* (14) adjusted six parameters involved in both the global polymerization rate coefficient and the micromixing time in order to match predicted and experimental polyethylene production obtained by homogeneous polymerization in a bench-scale CSTR. Afterwards Lorenzini *et al.* (4) presented a paper on the determination of model parameters and the adjustment of kinetic coefficients that affect molecular structure (molecular weights, short and long chain branching). Overall, their approach was similar to ours (1, 13). Nevertheless, they incorporated information about the entire MWD in the objective function. Their optimal values were in the range of previously published values. Lorenzini *et al.* (4) also presented an approach that was different from ours to force the model to fit data obtained under different experimental conditions. They linearized the model around an operating point by calculating the sensitivity matrix, whose elements are the sensitivity coefficients corresponding to model output related with kinetic parameters. Under certain operating conditions they run the model with the optimal reference kinetic set. They computed the difference between the model output and the experimental results in terms of relative errors and they used them in connection with the sensitivity matrix for the linearized model to obtain the corresponding kinetic parameter variation. They found that the results of the new model were in accordance with experimental data.

In this context, a study of the adjustment of a mathematical model to plant data is presented here. Our objective is to simplify the necessary periodic adjustment of model parameters by reducing a previous model in order to diminish the number of parameters to be adjusted and by developing shortcuts to hasten the adjusting process.

A rigorous mathematical model for multiple peroxide and oxygen initiator systems was previously developed by our research team (1). In this paper, this model is called the detailed model (DM). Once the model had been developed, its complete set of kinetic parameters was adjusted through a computationally laborious nonlinear regression using a given range of experimental data from an industrial tubular reactor. The following aspects of the DM model are reviewed here: reactions included in the kinetic mechanism, jacket temperature and pressure calculations, flow patterns and periodic pressure pulses. We propose considering constant jacket temperature and pressure at each reactor zone as well as a linear variation of reaction pressure without pulses. Each one of the model modifications that we suggest was tested against detailed model predictions and/or experimental data.

With respect to the reaction mechanism, we propose that only the reactions considered crucial to describe this polymerization should be kept as adjustable parameters. The others may even be eliminated from the reaction mechanism. A set of model runs was designed in order to determine which reactions from the DM model did not affect model outputs significantly.

We also analyzed the importance of each one of the steps of the oxygen initiation mechanism proposed in our former model (1). Such model included three

oxygen related reactions, as follows: reaction of oxygen with a monomer molecule to give an initiation radical, formation of a high-temperature peroxide by reaction of oxygen with a macroradical and finally, decomposition of such peroxide into an initiation radical at high temperature. In the present work, experimental runs with oxygen as unique initiator were used to analyze the incidence of all these reactions on model results. This allows us to determine the validity of this initiation model and to estimate the kinetic constants for the oxygen initiation independently.

As we stated in our previous work (1), the kinetic parameters estimated for each component of the peroxide initiator mixture were highly correlated. This also holds for the solvent mixture. In view of that, the initiator and solvent mixtures are treated here as a fictitious unique initiator and solvent respectively, with the same global molar concentration as the corresponding mixture. Experimental runs performed with different peroxide and solvent mixtures were used to estimate the related kinetic constants. A procedure was established for the quick estimation of kinetic parameters which were representative of initiator and solvent mixtures of different compositions. This resulted in a model that can be quickly updated to predict the behavior of a given industrial reactor.

FROM THE DETAILED MODEL (DM) TO THE FINAL REDUCED MODEL (FRM)

A diagram of a typical industrial LDPE tubular reactor is shown in *Fig. 1*. It is usual to find multiple feedings of monomer (M) as well as multiple injections of initiators (O_2, I_k) and chain transfer agents (S_k) at different locations through the axial length. The possible flux configurations are counter- and/or co-current. The jacket fluid may come from either the source water tank or any other jacket zone. Variations in jacket temperatures (Tj) and pressures (Pj) are observed along the axial length in these reactors. Pressure pulses are often used to clean reactor walls from polymer buildups. A detailed model (DM), which took into account all the above mentioned operating and design conditions, has already been reported (1). Its implementation included several iterative calculations because some of the operating variables were known at the reactor inlets while others, such as jacket temperatures and pressures for counter-current flow, were only known at the end of each reactor zone. Besides, pressure pulse was measured only at the reactor exit. In consequence, the model equations were solved by means of the shooting method applied in three successive stages. First, the pulse pressure drop, jacket temperature and jacket pressure at the reactor inlet were guessed. Then, the reactor equations were solved at the first reactor zone by means of the shooting method, checking jacket pressure only. Once convergence had been achieved the same procedure was applied, this time checking the jacket temperature. All the reactor zones were solved in the same way. At the reactor outlet the pulse pressure drop was checked. The entire procedure was repeated all over again until convergence to the desired accuracy was achieved for all the variables.

With respect to the kinetic constants, some were taken from literature data while the others were obtained through a laborious fit to experimental data, which implies several adjustable parameters. More information on the detailed model can be found elsewhere (1). In the rest of this section, we describe the path from the DM model to the final reduced model (FRM), which results from an exhaustive analysis of the hypotheses, the DM implementation and the parameter regression procedure.

The following basic hypotheses and features of the DM model were kept in the FRM model: plug flow, reaction mixture forming a single supercritical phase, variation of physical and transport properties along the axial length and use of heat transfer equations developed for the present reactor (15). As a first step to reduce the DM model, the jacket conditions were simplified as follows: pressure and temperature were considered constant through each jacket zone and equal to those of the corresponding source, either a tank or another jacket zone. Then, no discrimination between counter- or co-current flow would be necessary. In this way we eliminate the associated iterative calculations.

To analyze the importance of including periodic pressure pulses in the model, the pressure (P) along

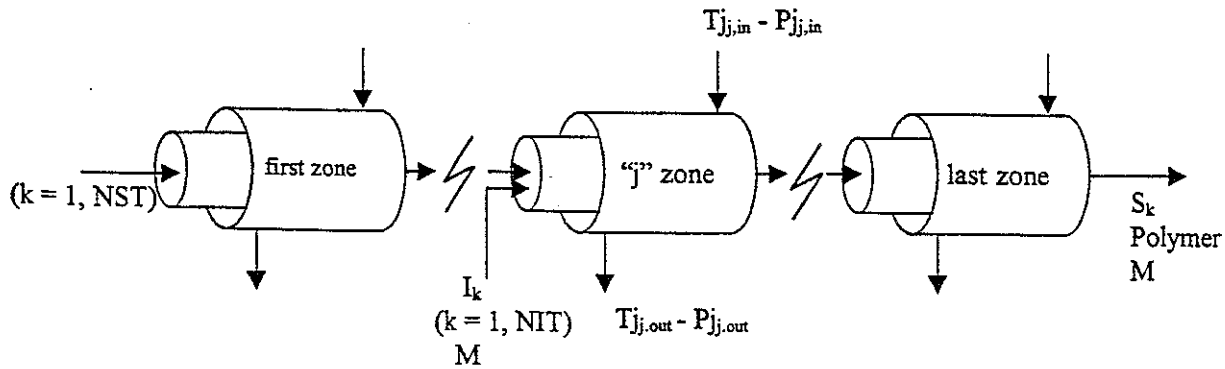

Fig. 1. Tubular reactor for the ethylene polymerization.

53-122

the reactor was described by a linear equation ($P = P_{inlet} - \Delta P_{fr} z$), thus eliminating the corresponding iterative calculations. This hypothesis did not work well, especially after the second initiator injection. The errors in temperature, conversion and property predictions increased significantly. This was to be expected because the pulse valve is located near the end of the reactor, so the pulse travels counter flow with respect to the reaction mixture. The pulse effects must be larger in the second zone, so the error ensues from disregarding the pulse is higher in such zone. In consequence, we recommend keeping the pressure pulse calculations, as was done in our DM model (1).

With respect to the reaction mechanism, the basic reactions for the free radical polymerization are initiation, propagation and termination. In the case of polyethylene, the accepted common termination is the combination of free radicals. Thermal degradation, which is equivalent to a β-scission, is one of the reactions that allows good prediction of temperature profiles (6). Transfer to polymer does not affect temperature profiles directly, but it allows the prediction of the high polydispersities found in this reactor as well as long-chain branching. We considered all the above mentioned reactions in the FRM model. Through several simulations performed with the DM model, we determined that temperature profiles and product properties did not change significantly for the present reactor when transfer to monomer, thermal initiation and double bond end propagation were removed from the mechanism. Then, they could be eliminated from a new general regression procedure or even from the mechanism. Only thermal initiation must necessarily be kept because it becomes important at runaway operation, which occurs at temperatures which are higher than the usual ones.

A simplified mechanism is also proposed in the FRM model to explain the unique oxygen initiation behavior. In the DM model, the particular shape of the temperature profiles at the peak when oxygen is employed was explained through the initiation by a high temperature peroxide produced by reaction of oxygen with macroradicals. That mechanism was analyzed here by using experimental data from oxygen initiated reactions as described below. This led to a simplified oxygen mechanism composed only by initiation with oxygen and reaction of oxygen with macroradicals to give an inert macromolecule.

When considering a multiple peroxide injection reactor, each one of the peroxide mixtures is proposed to be treated as a single fictitious initiator with only one kinetic constant to be adjusted. It was considered that one mixture was not equal to another one when it had a different composition either in peroxide components or just in its weight fraction composition. The fictitious initiator molar concentration must be equal to the sum of the molar concentration for each component. Mass flow and the corresponding molecular weight of each peroxide mixture were calculated as shown in *Eqs 1* and *2*.

$$Fin_{f,J} = \sum_{k=1}^{NIT} Fin_{k,J} \quad j = 1,NMEZIT \tag{1}$$

$$Min_{f,J} = \frac{Fin_{f,J}}{\sum_{k=1}^{NIT} Fin_{k,J}/Min_k} \quad j = 1,NMEZIT \tag{2}$$

With respect to the solvent mixtures we have also defined a fictitious solvent, which is fed at the same global molar flow rate as its corresponding mixture. The global molar flow rate and molecular weight of each solvent mixture were calculated using *Eqs 3* and *4*.

$$Fs_{f,J} = \sum_{k=1}^{NST} Fs_{k,J} \quad j = 1,NMEZSOL \tag{3}$$

$$Ms_{f,J} = \frac{Fs_{f,J}}{\sum_{k=1}^{NST} Fs_{k,J}/Ms_k} \quad j = 1,NMEZSOL \tag{4}$$

The reactions included in the FRM model are presented in *Eqs 5* to *16*.

Oxygen Initiation:

$$0_2 + M \xrightarrow{k_o} 2R_{1,0} \tag{5}$$

Generation of Inert:

$$0_2 + R_{i,x} \xrightarrow{f_o k_o} X \tag{6}$$

Peroxide Initiation:

$$I_{f,J} \xrightarrow{f_{f,J} k d_{f,J}} 2R_{1,0}$$

where

$$[I_{f,J}] = \sum_{k=1}^{NIT} [I_k]; j = 1, NMEZ \tag{7}$$

Monomer Thermal Initiation:

$$3M \xrightarrow{f_{mi} k_{mi}} R_{1,1} + R_{1,2} \tag{8}$$

Propagation:

$$R_{i,x} + M \xrightarrow{k_p} R_{i,x+1} \tag{9}$$

Termination by Combination:

$$R_{i,x} + R_{j,y} \xrightarrow{k_{tc}} P_{i+j-1,x+y} \tag{10}$$

Termination by Thermal Degradation:

$$R_{i,x+1} \xrightarrow{k_{tdt}} P_{i,x} + R_{1,0} \tag{11}$$

Chain Transfer to Polymer:

$$R_{i,x} + P_{j,y} \xrightarrow{k_{trp}} P_{i,x} + R_{j+1,y} \tag{12}$$

Chain Transfer to Solvent:

$$S_{f,1} + R_{i,x} \xrightarrow{k_{trs\,f,1}} P_{i,x} + R_{1,0} \text{ where } [S_f] = \sum_{k=1}^{NST} [S_k] \tag{13}$$

53-123

Backbiting: $$R_{t,x} \xrightarrow{k_{bb}} R_{t,x} \quad (14)$$

β-Scission to Secondary Radical:

$$R_{t,x+1} \xrightarrow{k_{\beta 1}} R_{1,0} + P_{t,x} \quad (15)$$

β-Scission to Tertiary Radical:

$$R_{t,x+1} \xrightarrow{k_{\beta}} R_{1,0} + P_{t,x} \quad (16)$$

Mass and energy balance equations for the present reactor, which take into account all the considerations mentioned above, are presented in *Eqs 17* to *20*.

Mass Balances for Components and Moments

$$\frac{d[C_j]}{dz} = -\left(r_j + [C_j]\frac{dv}{dz}\right)/v; [C_j] = [O_2],[M],[I_k]k = 1..NT,\ [S_k]k = 1..NST,\ [\lambda_{m,n}],[\mu_{m,n}],m = 0,1;\ n = 0,1,2;\ [Me],\ [Vi],\ [Vd] \quad (17)$$

Reactor Temperature

Heating and Reaction Zones

$$\frac{dT}{dz} = \frac{1}{\rho C_p v}\left(\frac{4U(T - Tj)}{D_t} + f_h k_p \lambda_{0,0}[M](-\Delta H)\right) \quad (18)$$

Friction Pressure Drop $$\frac{dP}{dz} = -\rho\left(v\frac{dv}{dz} + \frac{2f_r v^2}{D_t}\right) \quad (19)$$

Pulse Valve Effects

$P = P_{ft} + \Delta P_{pv_i} e^{-\delta(t-t_p)}$ *where*

$$\Delta P_{pv_i} = \Delta P_{pv_{i-1}}\left(1 + \gamma\left(\frac{P_{f_i} - P_{f_{i-1}}}{P_{f_{i-1}}}\right)\right) \quad (20)$$

Kinetic constant values for propagation (k_p), monomer thermal initiation (k_{mi}), termination by combination (k_{tc}), thermal degradation (k_{tdt}), transfer to polymer (k_{trp}), backbiting (k_{bb}) and the β-scissions ($k_{\beta 1}$ and k_β) were the same as those previously reported (1). Kinetic parameters related to the oxygen, fictitious peroxides and solvent were determined as described below.

The FRM model was implemented in Fortran code using standard numerical routines for stiff ordinary differential equations, just as it was done in the DM model (1). The main profiles provided by the FRM program as function of axial length are: conversion (X); reaction temperature (T) and pressure (P); mass fraction of all components; the first three moments for the combined length and branching distributions of radicals and polymer; linear rate (v), number and weight average molecular weights (Mn and Mw) and short and long chain branching indexes.

Analysis of the Oxygen Mechanism

First, simulations were performed assuming that the only initiation reaction present was the initiation by oxygen (*Eq 5*), whose kinetic constant is k_o. For each fixed value of the pre-exponential factor (A_o) in k_o, a scanning of the corresponding activation energy (E_o) was carried out. The objective function SSQ_k (in this case k = o) was calculated each time by means of *Eq 21*. The values of E_o that minimized that objective function were kept in memory.

$$SSQ_k = \sum_{i=1}^{N_c}\sum_{j=1}^{N_{exp}}\left|\frac{T_c^{(i}(j) - T_{exp}^{(i}(j)}{T_{exp}^{(i}(j)}\right|^2 \quad (21)$$

Afterwards, we included the reaction of oxygen with a radical, which generates an inert or eventually a high temperature peroxide (*Eq 6*). For each set of local optima (A_o, E_o) found in the previous step we obtained the corresponding optimum value for the proportional factor (f_o) for this second reaction, by minimizing the same objective function (*Eq 21*). Finally, a third reaction was incorporated to the adjustment, taking into account the possibility of initiation by the high temperature peroxide (1). The kinetic constant for the decomposition of the high temperature peroxide was taken from previous work (1). Only the reaction's efficiency (f_{PO2}) was incorporated as an adjustable parameter. In this case, for each set of local optima (A_o, E_o, f_o) we followed the same procedure as in the previous step to obtain the local optimum f_{PO2}.

We analyzed the accuracy of the temperature adjustment obtained at each stage, determining the minimum level of complexity necessary to describe the oxygen mechanism in order to predict temperature profiles adequately. The conversion and polydispersity were also considered in this analysis.

Method for Determination of the Kinetic Parameters Related to the Fictitious Initiators and Solvents

First, the feasibility of treating each one of the initiator and solvent mixtures as a fictitious single component was determined by means of a parametric study on the corresponding kinetic constants. It was possible to obtain temperature profiles, molecular properties and conversions of the same order as the experimental ones. In a second stage, the optimum values for the kinetic parameters of the fictitious components were estimated from a non-linear regression.

When adjusting the fictitious initiator parameters, we employed the objective function shown in *Eq 21*, since the initiator and its concentration mainly affect the temperature profiles (in this case k = in1, in2,..). The regression variable was the activation energy of the fictitious initiators ($Efin_j$) of each one of the "j" initiator mixtures for a given pre-exponential factor ($Afin_j$). The starting value of each $Efin_j$ was determined from the expression in *Eq 22*, evaluated at a fixed temperature so as to have a value for the activation energy, given the pre-exponential factor.

53-124

$$f_{f,j}\, kd_{f,j}[I_f] = \sum_{k=1}^{NIT} f_k\, k_{d_k}[I_k] \qquad (22)$$

On the other hand, the polymer's molecular weight is the property that was affected by changes in the chain transfer to solvent kinetic constant. So, we selected the following objective function (*Eq 23*) to perform the corresponding regression:

$$SSQ_{sj} = \sum_{i=1}^{Nc} \left| \frac{Mn_c^{(i} - Mn_{exp}^{(i}}{Mn_{exp}^{(i}} \right|^2 + \left| \frac{Mw_c^{(i} - Mw_{exp}^{(i}}{Mw_{exp}^{(i}} \right|^2 \qquad (23)$$

The variable under adjustment was the activation energy of the fictitious solvent (Efs_j) of each one of the "J" solvent mixtures for a given value of the pre-exponential factor (Afs_j). The starting value for Efs_j was the same as the major component of the solvent mixture, taken from (1).

Several runs using oxygen and a solvent mixture (*NMEZSOL* = 1) in the main feed plus two lateral injections of peroxide mixtures (*NMEZIT* = 2), were employed in the regressions. The main details of the regression procedure are explained below.

First, a minimization of *Eq 21* was performed. It was done using only the kinetic parameters of the first peroxide mixture as optimization variables, employing temperatures measured up to the end of the first reaction zone. Once a set of parameter values had been determined the second reaction zone was adjusted by minimizing *Eq 21* using the values of the kinetic parameters that corresponded to the second mixture as optimization variables. In this case, only the information corresponding to the second reaction zone was considered in the adjustment. Finally, the kinetic parameters of the chain-transfer to solvent reaction were employed to minimize *Eq 23*.

For each stage, the procedure employed to fit the kinetic parameters consisted in finding the value of $Efin_j$ or Efs_1 which minimizes the corresponding objective function SSQ_{inj} or SSQ_{sj}, for different values of pre-exponential factor $Afin_j$ (j = 1,NMEZIT) or Afs_j (j = 1,NMEZSOL), afterwards selecting the global minimum. The adjustment of each pre-exponential factor/activation energy pair was not attempted simultaneously because overflows are produced for certain combinations of such parameters, which leads to runaway situations.

In all cases it was found out that the activation energy vs. log (pre-exponential factor) is a straight line for the combinations ($Afin_j$, $Efin_j$) or (Afs_j, Efs_j), which resulted in a minimum. It was also observed that all the kinetic constants corresponding to these points coincide at one temperature. The computational time required to fit the parameters was reduced considerably by taking advantage of the above mentioned feature. Once the straight line has been obtained with a few points, the value of the activation energy which will give a minimum for other pre-exponential factors can be read directly from a plot. So, it is only necessary to run a single simulation for each pair of values to get the minimum SSQ for that pre-exponential factor.

This approach allowed us a reduction in the number of kinetic parameters of initiator and solvents to be adjusted from 2(*NST* + *NIT*) to only 2(*NMEZIT* + *NMEZSOL*).

EXPERIMENTAL INFORMATION

The experimental data that we employed to analyze the oxygen mechanism had been previously reported in Brandolin *et al.* (13) as "Reactor A." They belonged to a single feed industrial reactor, where it was only used oxygen as initiator. *Table 1* shows the operating conditions used for the peroxide and solvent adjustments. These runs were performed in the same reactor, but using oxygen in the main feed as well as two injections of peroxide mixtures, which led to two reaction zones. Mass flow rates, temperatures and pressure relative to the operating conditions for Case 1, are reported as function of their location at the reactor, expressed with respect to the total reference length of the reactor. In all runs, the weight composition of the first peroxide mixture was: 42% initiator A, 26% initiator B, 14% initiator D and 18 % initiator E. The second initiator injection was composed of: 36% initiator C, 48% initiator D and 16% initiator F. The weight composition of solvent mixtures considered in this work was: 89–97% of solvent A, up to 10% of solvent B and up to 4% of solvent C.

Average molecular weights and long chain branching indexes were determined by means of gel permeation chromatography (GPC) in a Waters-150-C ALC-GPC. Global short chain branching are reported as the sum of methyl, vinyl and vinylidene groups in polyethylene samples, which were determined by infrared spectroscopy using a FTIR-Nicolet 520. The conversions were calculated from measured monomer mass rates at the reactor entrances and polymer mass rate after the separation stages.

RESULTS AND DISCUSSION

The relevance of the oxygen related reaction mechanisms is discussed first. *Figure 2a* shows the pre-exponential factor (Ao) of the oxygen decomposition into initiation radicals as a function of the activation energy (Eo) that minimizes the objective function SSQ_o (*Eq 21*). It appears that such points are connected by a straight line, so the simplified regression procedure is applicable in this case. The corresponding minimum SSQ_o (●) is also plotted in *Fig. 2a*. Besides, this figure presents the minimum SSQ_o obtained when the oxygen reaction with macroradicals that gives an inert (◇) is added to the mechanism. In this case the adjustable parameter was the factor f_o that multiplies the base value of the kinetic constant for this reaction.

53-125

Table 1. Operating Conditions for Runs 05, 06, and 10. Relative Values With Respect to Those of Run 01 are Reported.

Input Mass Rates	z/z_{ref}	Run No. 05	06	10
Monomer	6.25×10^{-3}	1.01	1.00	1.00
Oxygen	6.25×10^{-3}	0.97	0.85	1.00
Peroxide A	0.10	0.87	0.71	1.09
Peroxide B	0.10	0.86	0.71	1.09
Peroxide C	0.53	1.09	0.78	1.51
Peroxide D	0.10	0.87	0.71	1.09
	0.53	1.09	0.78	1.51
Peroxide E	0.10	0.87	0.71	1.09
Peroxide F	0.53	1.09	0.78	1.51
Solvent A	6.25×10^{-3}	0.51	0.45	1.57
Solvent B	6.25×10^{-3}	0.66	0.65	1.65
Solvent C	6.25×10^{-3}	1.10	1.08	1.04
Jacket Fluid (water)	0.21, 0.34, 0.42, 0.50, 0.59, 0.71, 0.84	1.05, 1.30, 1.06, 1.09, 1.10, 1.03, 1.07	1.00, 0.81, 1.01, 1.03, 1.03, 0.97, 1.03	1.06, 1.31, 1.01, 1.00, 1.00, 1.00, 1.00
Pressures				
Inlet Pressure	6.25×10^{-3}	1.00	1.00	1.00
ΔP_{pulse}	0.84	1.00	0.91	1.00
t_p	—	1.00	0.96	1.00
t_r	—	0.91	0.91	0.95
Jacket Pressures	0.21, 0.34, 0.42, 0.50, 0.59, 0.71, 0.84	1.06, 1.00, 0.93, 1.00, 1.00, 0.93, 0.93	1.05, 0.89, 1.04, 0.89, 0.89, 1.04, 1.04	1.04, 0.99, 1.00, 0.99, 0.99, 1.00, 1.00
Temperatures				
Inlet Temperature	6.25×10^{-3}	0.99	0.93	1.00
Vapor Temperature	3.75×10^{-2}	0.98	1.00	1.00
Water Temperature	0.21, 0.34, 0.42, 0.50, 0.59, 0.71, 0.84	1.01, 0.97, 0.95, 0.98, 0.98, 0.95, 0.96	1.02, 1.04, 0.99, 1.04, 1.04, 0.99, 0.99	1.00, 1.00, 1.00, 1.00, 1.00, 1.00, 1.00

When considering the generation of a high temperature peroxide and its decompositions no significant improvement was observed in the SSQ_o values. It is clear from *Fig. 2a* that the errors are significant in the profiles obtained by assuming only oxygen decomposition into initiation radicals (*Eq 5*), at least up to a value of Eo = 34,500 cal/mol. For larger values of Eo, the values of objective function SSQ_o are similar for all the assumptions. *Figure 2b* shows temperature peak values vs. their location, while *Fig. 2c* shows polydispersity (PD) vs. monomer conversion (X). These results correspond to simulations done using the set of values for (Ao, Eo) or (Ao, Eo fo), whichever applies in each option, that produces a local minimum in SSQ_o. All the predicted values are reported with respect to the corresponding experimental ones, so the best prediction coincides with a coordinate equal to one. It becomes evident that it is impossible to predict the position and value of the peak temperature appropriately under the assumption that oxygen decomposes into initiation radicals only for any combination of activation energy with pre-exponential factor. In contrast, the addition of the reaction of oxygen with macroradicals to give an inert allows a good prediction of the temperature peak location and value. These considerations are also valid for polydispersity and conversion, as shown in *Fig. 2c*. No significant improvements in the predictions were detected by including the initiation by a high temperature peroxide derived from oxygen.

53-126

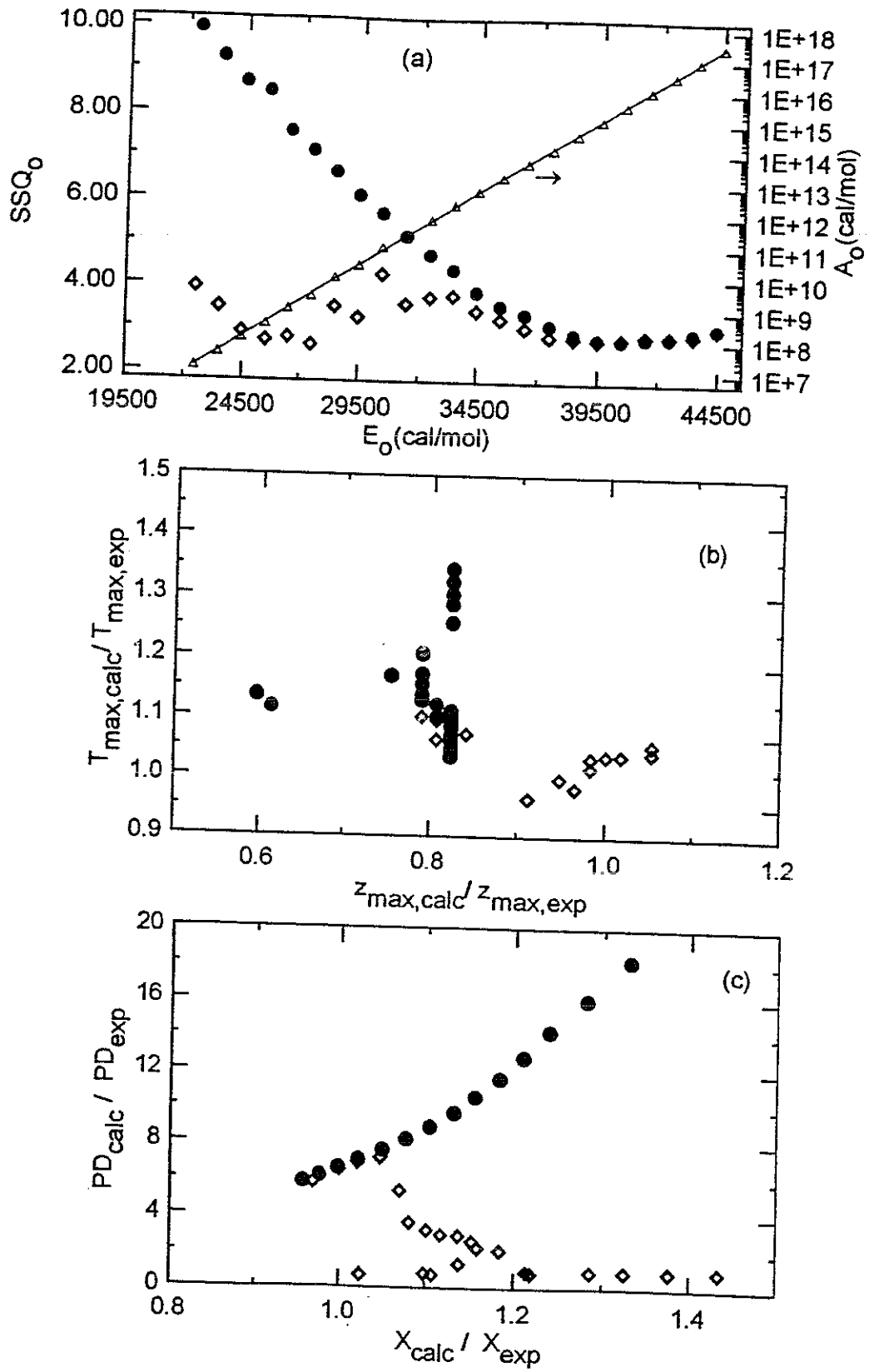

Fig. 2. Oxygen mechanism. (a) Oxygen objective function SSQ_o and pre-exponential factor of oxygen decomposition into radicals (Δ) vs. the corresponding activation energy. (b) Ratio of calculated to experimental maximum temperatures vs. ratio of calculated to experimental location of maximum temperatures. (c) Ratio of calculated to experimental polydispersities vs. ratio of calculated to experimental conversions. ● Oxygen decomposition into radicals (Eq 1), ◇ Including decomposition to inert (Eqs 1 and 2).

S3-127

Table 2. Kinetic Parameters for the Initiation Mechanisms of the FRM Model.

Parameter	Value
Ao	2.75×10^{10} $L^{1.1}/mol^{1.1}s$
Eo	29,465 cal /mol
fo	fo = 2.01 10^7
$Efin_1$	22,200 cal/mol
$Afin_1$	$1. \times 10^9$ 1/s.
fin_1	0.9
$Efin_2$	9200 cal/mol
$Afin_2$	$1. \times 10^5$ 1/s.
fin_2	0.9
Efs_1	4,121 cal/mol
Afs_1	$7. \times 10^4$ 1/mol s.

Table 2 presents the optimum kinetic values obtained for the oxygen mechanism. As an example, *Fig. 3* shows the experimental and calculated temperature profiles obtained using these optimum kinetic values for the operating conditions already reported for "Reactor A" (13). Good prediction of properties and conversion was achieved by only including the generation of an inert. For example, PD_{calc}/PD_{exp} = 0.85 and X_{calc}/X_{exp} = 1.09.

From the analysis described above it can be stated that the usual mechanisms of oxygen initiation do not allow a good prediction of the industrial temperature profiles. It is possible to improve the prediction greatly with the mere addition of an equation for the consumption of oxygen by reaction with free radicals to give an inert.

We also employed data from a two injection reactor (see *Table 1*) to test our proposed reduced initiation mechanism for the peroxide mixtures. The starting values for the fictitious initiator activation energies in the regression procedure were calculated from *Eq 22*. The initiator mixture efficiencies were fixed arbitrarily (see *Table 2*). *Figure 4a* shows the plot of the pre-exponential factor ($Afin_1$) and the objective function SSQ_{in1} vs. the activation energy ($Efin_1$) that minimizes the SSQ_{in1} function for the first reaction zone, considering all the temperature measurements up to the first peak, plus a few experimental points located immediately after it. Measurements corresponding to the cooling zone were not included in the adjustment since in such case the optimized kinetic parameters could only incorporate information that corresponded to the heat transfer between the reaction mixture and the jacket fluid. *Figure 4a* shows that the optimum sets ($Afin_1$, $Efin_1$) are related by a straight line, thus allowing the use of the simplified regression procedure explained above. The plot of local minimum SSQ_{in1} vs. $Efin_1$ indicates that this is not a smooth function; so, special care should be taken to find out the global minimum. *Figure 4b* shows the calculated first peak

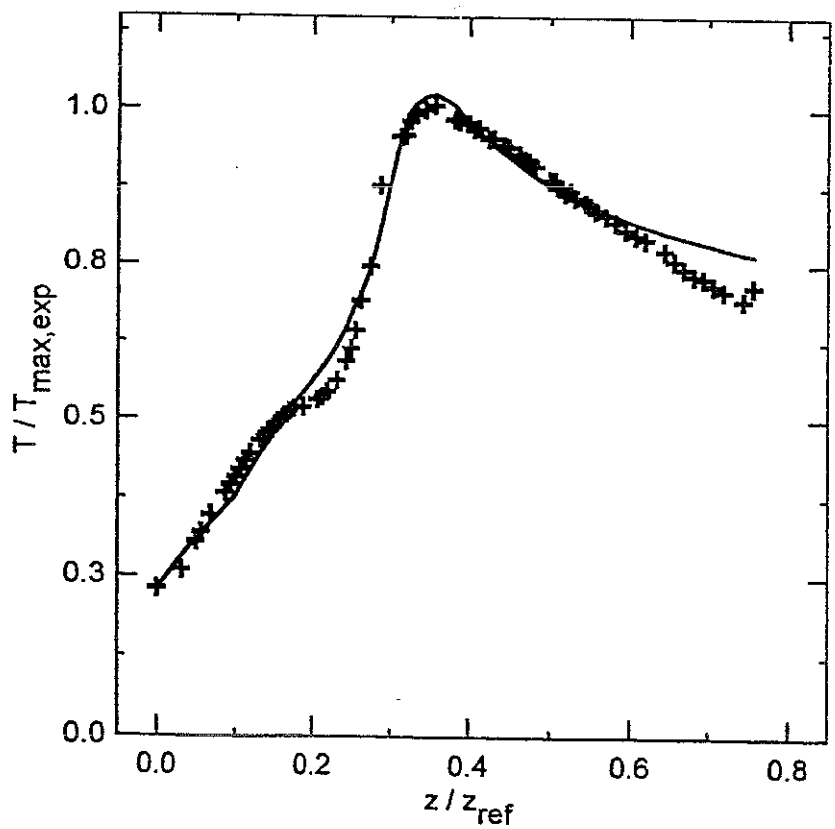

Fig. 3. Experimental (+) and calculated (——) temperature profiles for "Reactor A" (13). obtained with the optimum oxygen mechanism.

53-128

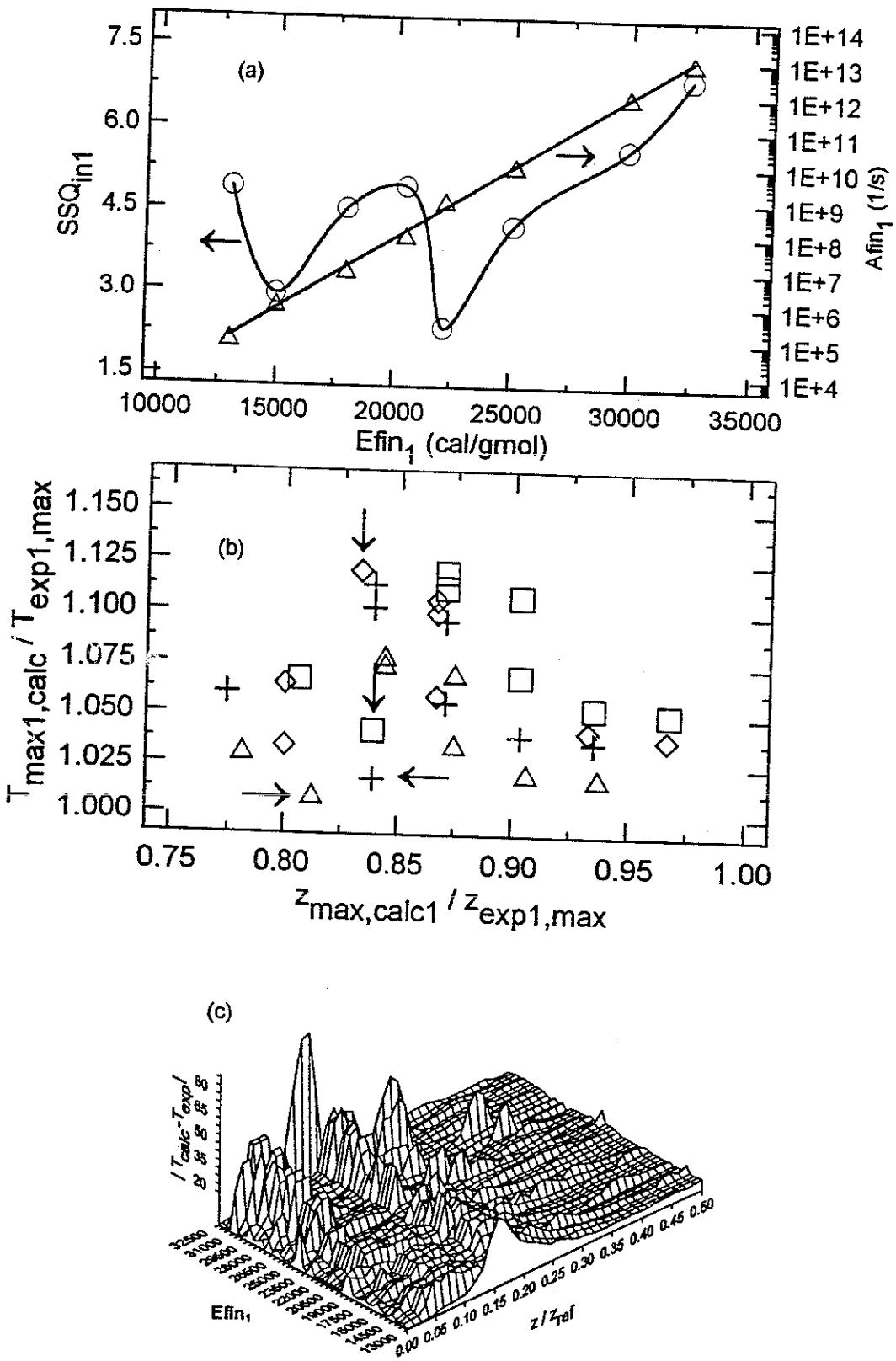

Fig. 4. Fictitious initiator mechanism for the first peroxide mixture. (a) Objective function SSQ_{in1} (○) and pre-exponential factor of fictitious initiator decomposition (△) vs. the corresponding activation energy. (b) Ratio of calculated to experimental location of first maximum temperatures vs. ratio of calculated to experimental first maximum temperatures for runs 1 (+), 5 (□), 6 (△), and 10 (◇). (c) Difference between calculated and experimental temperatures vs. first fictitious activation energy and ratio of axial length to total reference length.

53-129

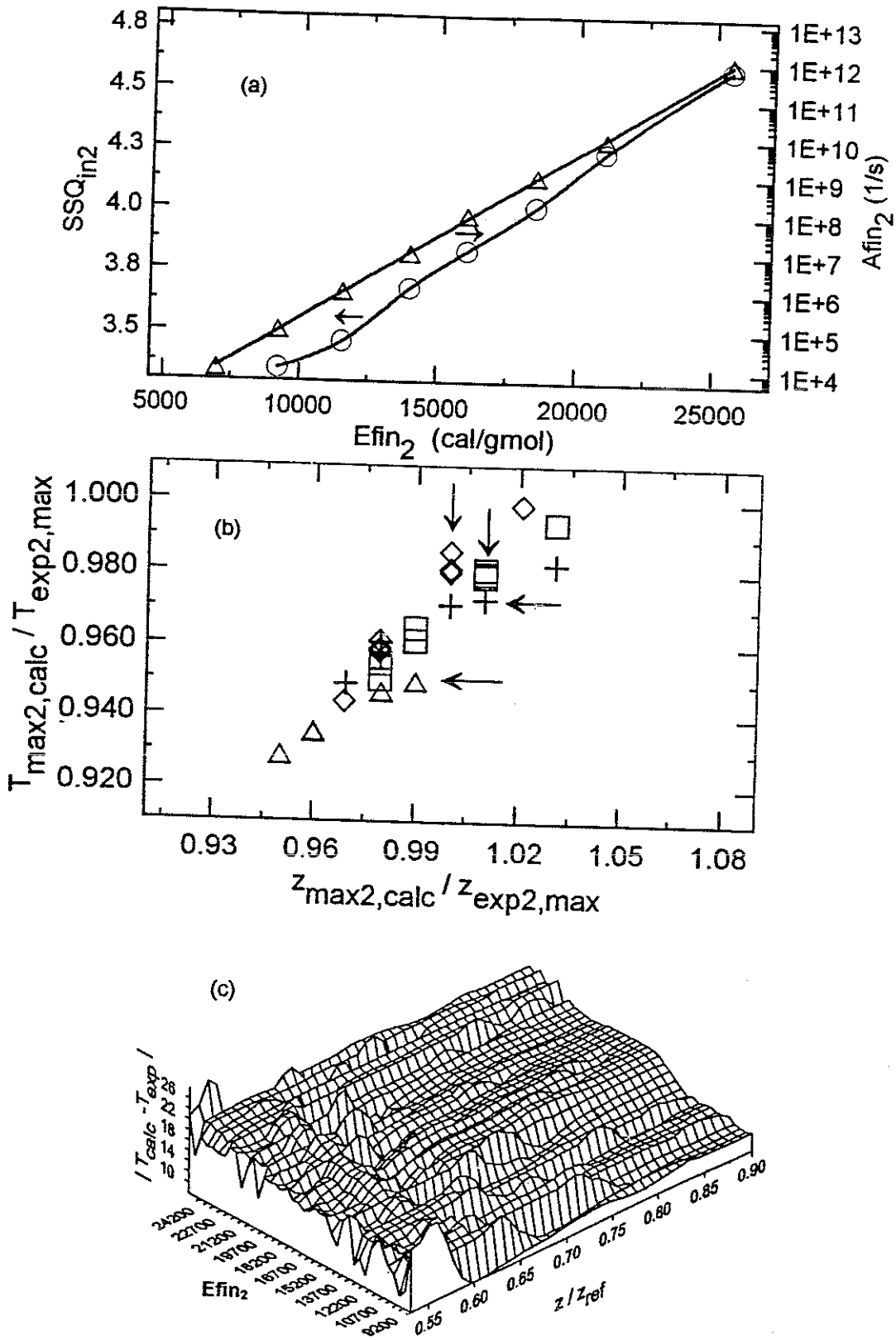

Fig. 5. Fictitious initiator mechanism for the second peroxide mixture. (a) Objective function SSQ_{in2} (○) and pre-exponential factor of fictitious initiator decomposition (△) vs. the corresponding activation energy. (b) Ratio of calculated to experimental second maximum temperatures vs. ratio of calculated to experimental location of second maximum temperatures for runs 1 (+), 5 (□), 6 (△), and 10 (◇). (c) Difference between calculated and experimental temperatures vs. second fictitious activation energy and ratio of axial length to total reference length.

temperature vs. its calculated position, for the combinations of optima ($Afin_1$, $Efin_1$) which produce a local minimum in $SSQin_1$, for all the runs presented in *Table 1*. The arrows point out the global optimum for each run. It should be noted that the global optimum ($Afin_1$, $Efin_1$) is the one that produces the best approximation to the experimental profiles for $z/z_{ref} < 0.3$. So, it is not surprising that the pair ($Afin_1$, $Efin_1$) that produces a global minimum in SSQ_{in1} may be different from the one by which the location and value of the peak temperatures are best predicted. *Figure 4c* presents the difference between calculated and experimental temperatures of run 10 vs. the axial length, for each pair of local optima ($Afin_1$, $Efin_1$), which are identified by $Efin_1$ in one of the axis. Because of the steep slope of the temperature profiles when approaching the peak, a slight deviation in the location of the predicted temperature profile with respect to the experimental profile leads to differences between calculated and experimental temperatures for the same axial position that are significantly above the experimental measurement error.

For the second reaction zone, similar results are shown in *Figs. 5a, b* and *c*. The global optimum values of $Afin_1$ and $Efin_1$ for the first zone were used (see *Table 2*). We obtained the expected straight line relating $Afin_2$ and $Efin_2$, which produced a local minimum in SSQ_{in2} (*Fig. 5a*); so, the simplified regression was applied in this case. *Figure 5b* also indicates that a good prediction of position and value of the second peak temperature has been obtained. *Figure 5c* shows the differences between calculated and experimental temperatures for run 10 at the second reaction zone ($0.53 < z/z_{ref} < 0.84$). The optimum values for the second fictitious initiator are shown in *Table 2*.

When analyzing the fictitious solvent hypothesis, *Eq 23* was used as objective function. To start the search of the optimum kinetic constant for chain transfer to solvent we used solvent A values reported in reference (1) since it was the major component of the solvent mixture. *Figure 6* shows the typical simplified regression procedure, applied in this case to obtain optimum sets (Afs_1, Efs_1). First, a scanning of Efs_1 was carried out for three values of Afs_1, thus obtaining the curves of SSQ_s vs Efs_1 (*Fig. 6a*). The Efs_1 and Afs_1 that corresponded to the minimum of each curve were plotted against each other (● symbols in *Fig. 6b*). Besides, a straight line that correlates log(pre-exponential factor) vs. activation energy was found using the least-squares technique ($R^2 = 0.999953$). Then, the simulation was run for other pairs of such kinetic parameters that lie in the straight line (◇ symbols in *Fig. 7b*), thus obtaining the corresponding minimum SSQ_s function. The global minimum gave us the kinetic parameters to be used for the fictitious solvent (see *Table 2*).

As an example, *Fig. 7* shows predicted temperature profiles by the DM and FRM models, compared with experimental data for run 10. The DM model fits the experimental temperature data very well. In the case of the FRM model, the prediction is also good but the roundness of the peak region was not reproduced at the first reaction zone. This must be due to the special combination of pre-exponential factor and activation energy necessary to obtain good temperature increases. The value of the fictitious activation energy for the first zone must be low enough to allow the start of the reaction at low temperatures and the pre-exponential factor must take a value that allows the reaction to reach the usual maximum temperatures of around 300°C. Instead, very good agreement between calculated and experimental temperatures was obtained in the second zone. The temperature jump in this reaction zone is lower than the one in the first zone, the assumption of only one fictitious initiator being more accurate.

Table 3 contains calculated results and errors for conversion, number and weight average molecular weights and long and short chain branching for both models and all the runs considered in *Table 1*. Relative errors are calculated with respect to the experimental value obtained for each run.

The molecular properties were not included in the adjustment of initiation parameters. It was found that the reduced model tends to overestimate the weight-average molecular weight and errors are higher than those produced by the DM model when the fictitious solvent hypothesis was not considered. In general, when this hypothesis was included, the error in molecular property prediction diminished. This hypothesis was not only a good representation of the solvent, but also allowed us to compensate errors due to other model assumptions.

In general, the FRM model is able to predict molecular properties in the same order of values as the detailed model. Number-average molecular weight, short and long chain branching are predicted within the experimental error. The conversion is also calculated appropriately. As expected, errors are higher when using the FRM model.

An important advantage of the FRM model is the reduction in CPU time with respect to those of the DM model. For example, the same run performed in a Pentium (350 MHz, 96 Ram) computer took around 48 s for the DM model and around 35 s for the FRM. In general, the simulation times are reduced by about 25% when incorporating the fictitious initiator and solvent hypotheses together with constant jacket temperature and pressure. Half of this drop may be attributed to the assumption of constant jacket temperature and pressure. The rest of the savings in CPU time is produced by the fictitious initiator and solvent assumptions. It must be noted that execution times fall well below the reactor's residence time, thus making the model attractive for on-line applications. Nevertheless, the most important point for eliminating those reactions is to reduce the magnitude of the parameter estimation problem.

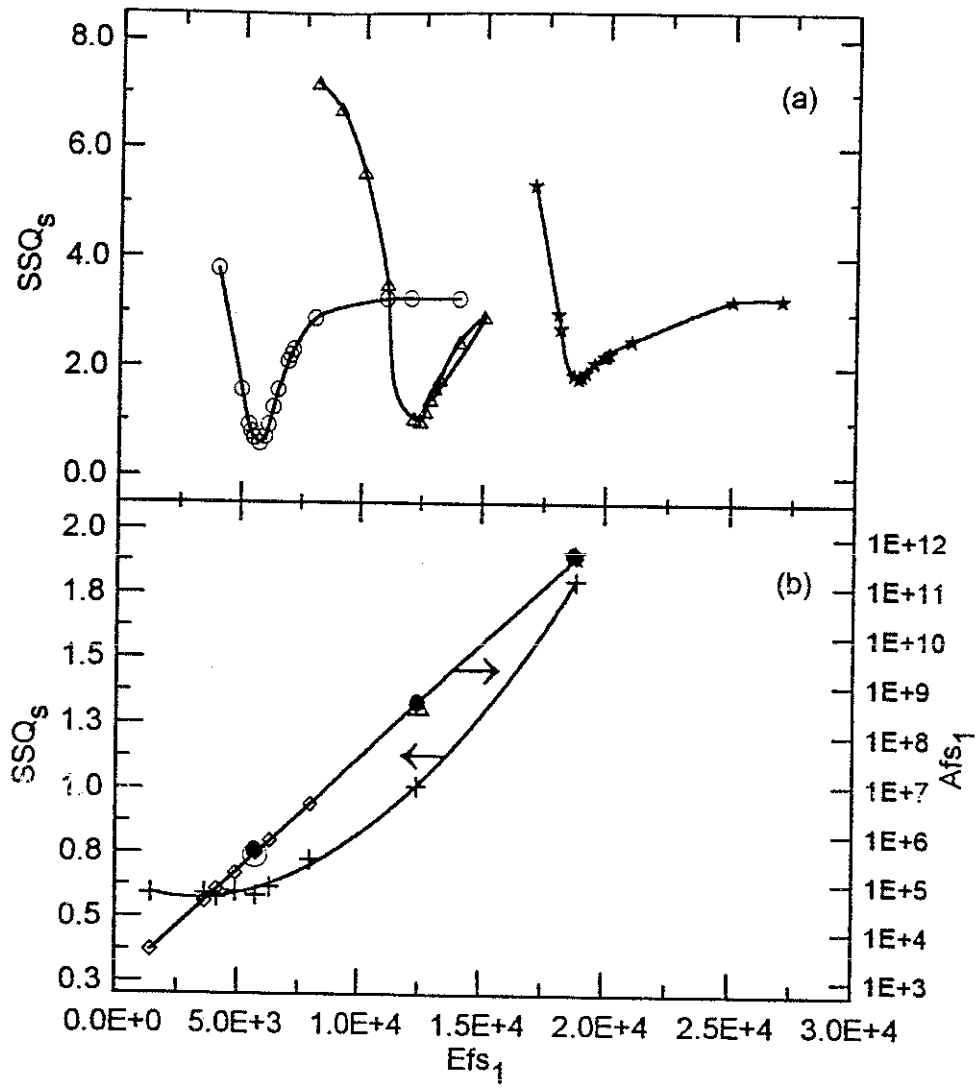

Fig. 6. Solvent mechanism. (a) Objective function SSQ_s (○): $Afs_1 = 7 \times 10^5$, △: $Afs_1 = 8 \times 10^8$, ★: $Afs_1 = 8.5 \times 10^{11}$) for different fictitious solvent pre-exponential factors vs. the corresponding activation energy. (b) Minimum solvent objective function SSQ_s (+) and the corresponding pre-exponential factor (◇, ●) vs. fictitious solvent activation energy.

CONCLUSIONS

A reduced model for the high pressure polymerization of ethylene in tubular reactors was validated in this work. Assumptions of different constant jacket temperature and pressure at each jacket zone and the elimination of transfer to monomer and double bond end propagation were appropriate for our reactor. It was important to keep pressure pulse calculations in the model. Fictitious initiator and solvent hypotheses work well for the range of operating conditions considered in this work.

The reduced model describes reactor behavior appropriately with fewer kinetic parameters than the DM model. This results in a simulator that may be updated quickly whenever the range of operating conditions changes.

With respect to the oxygen mechanism, data from polymerization initiated only with oxygen allows the assessment of the influence of each reaction on model outputs. It was determined that only one reaction of oxygen initiation did not permit a good prediction of temperature profiles typical of industrial reactors. The temperature and polydispersity predictions are notably improved by adding the consumption of oxygen by reaction with macroradicals to give an inert. The consideration of the generation of a peroxide instead of an inert, followed by peroxide initiating at high temperature did not improve model results. Then, it could be stated that when oxygen is added to the reaction mixture its initiation can be described by decomposition into initiation radicals and into inert species.

For runs performed with both oxygen and peroxide mixtures, the roundness of the peak was lost. In the

53-132

Table 3. Conversions Predicted by the Detailed Model and the Different Stages to Reach the Final Reduced Model. Relative Err
Were Calculated With Respect to the Corresponding Experimental Value [(calc. - exp.) / exp.].

Run		01		05		06		10	
Property	Model	value	error %	value	Error %	value	error %	value	error %
Conversion	DM	27.24	−2.05	27.44	6.69	25.89	3.23	28.14	−7.31
	FRM	25.84	−7.08	26.07	1.36	23.69	−5.54	27.52	−9.35
Mn	DM	22,343	−4.52	23,633	−5.09	24,600	0.00	19,692	0.98
	FRM	23,049	−1.50	25,319	1.68	27,143	10.34	20,126	3.21
Mw	DM	167,042	−2.83	192,967	0.87	198,090	3.67	136,385	−9.56
	FRM	171,309	−0.34	213,995	11.86	219,791	15.38	131,128	−13.05
LCB/1000C	DM	2.34	−0.85	2.35	4.44	2.17	−2.25	2.52	−2.70
	FRM	2.06	−0.85	2.05	−8.89	1.80	−18.92	2.32	−10.42
SCB /1000C	DM	24.60	7.84	24.39	3.88	23.65	−0.02	25.75	4.24
	FRM	23.80	4.34	23.04	−1.87	21.84	−0.10	25.45	3.02

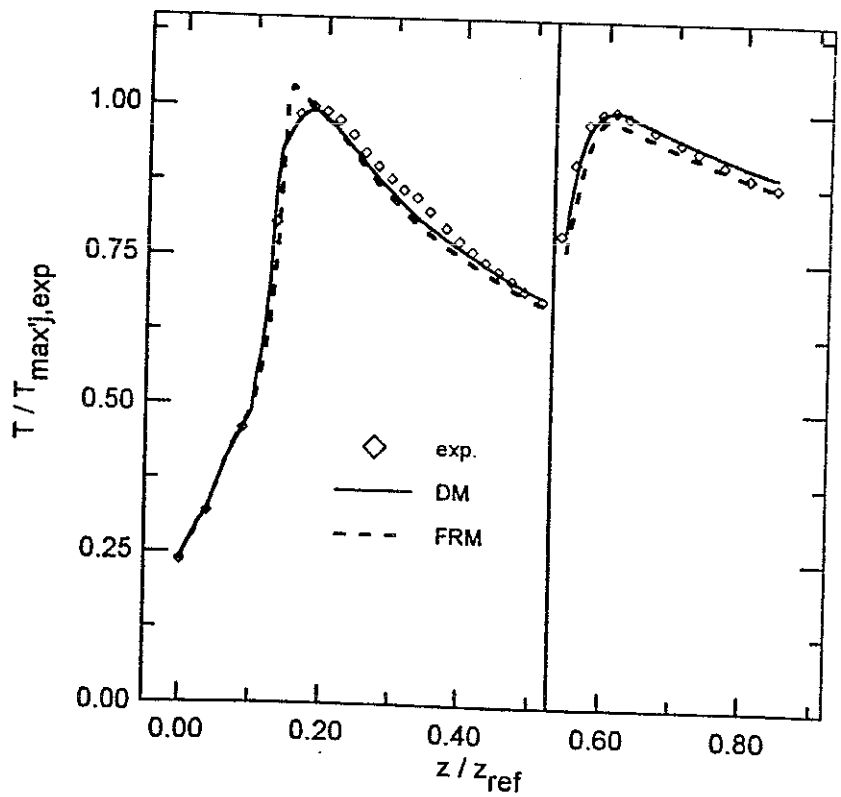

Fig. 7. Experimental and calculated temperature profiles for run 10. Operating conditions reported in Table 4.

53-133

DM model, this roundness was accomplished by the initiation at high temperature of peroxide derived from oxygen. Nevertheless, the runs performed with oxygen alone determined that such reaction did not affect model results. This high temperature peroxide may be present in the reactor, but it has not necessarily been derived from oxygen in the way that we previously had proposed. It could also be the result of an interaction between oxygen and peroxides. This issue requires further study.

Finally, it was determined that the kinetic parameters for fictitious initiators and solvents can be uniquely determined through the regression, provided the other kinetic parameters have been already determined. An efficient procedure to estimate the kinetic parameters that are representative of different initiator and solvent mixtures at different compositions was also established. Results presented here show the validity of the method.

ACKNOWLEDGMENTS

The authors gratefully acknowledge the financial support given by CONICET (the Argentinian National Research Council) and UNS (the National University of the South).

NOMENCLATURE

C_p	heat capacity of reacting mixture
D_i	reactor internal diameter
$Fin_{f,j}$	global initiator mass flow rate in the "j" injection
$Fin_{k,j}$	k^{th} initiator mass flow rate in the "j" mixture
$Fs_{f,j}$	global mass flow rate of "j" solvent mixture
$Fs_{,k,}j$	k^{th} solvent mass flow rate in the "j" mixture
f_k	efficiency of k^{th} peroxide initiator
$f_{f,j}$	eficiency of the j^{th} fictitious initiator
f_h	heating factor (1: reaction zone, 0: heating zone)
f_{mi}	efficiency of monomer thermal initiation
f_r	internal friction factor
$kd_{f,j}$	kinetic constant of the j^{th} fictitious initiator
kd_k	kinetic constant of the k^{th} initiator
$k_{trs,f,j}$	kinetic constant of the j^{th} fictitious solvent
$Min_{f,j}$	average molecular weight of "j" peroxide mixture
Min_k	molecular weight of "k" peroxide initiator
$Mn_c^{(i)}$	calculated number-average molecular weight for case "i"
$Mn_{exp}^{(i)}$	experimental number-average molecular weight for case "i"
$Ms_{f,j}$	average molecular weight of "j" solvent mixture
Ms_k	molecular weight of "k" solvent
$Mw_c^{(i)}$	calculated weight-average molecular weight for case "i"
$Mw_{exp}^{(i)}$	experimental weight-average molecular weight for case "I"
N_c	number of experimental cases used for the adjustment
N_{exp}	number of experimental temperatures for a given case study
$NMEZIT$	number of initiator mixtures
$NMEZSOL$	number of solvent mixtures
NIT	total number of peroxide initiators
NST	total number of solvents
P_{fi}	pressure at point "i" due to friction
P_{inlet}	pressure at reactor inlet
$P_{i,x}$	polymer with x monomer units and i long chain branches
$R_{i,x}$	radical with x monomer units and i long chain branches
r_j	"j" reaction rate
t	time in pressure pulse equations
$T_c^{(i)}(j)$	calculated temperature for case "i" at point "j"
$T_{exp}^{(i)}(j)$	experimental temperature for case "i" at point "j"
$T_{max\,j}$	temperature of the "j" peak
t_p	pulse time
t_r	pulse recovery time
U	global heat transfer coefficient
z	axial length
$z_{max\,j}$	location of the "j" peak
z_{ref}	reactor length for reference

Subscripts

$calc$	calculated
exp	experimental
in_j	j^{th} first fictitious initiator (j = 1, 2)
$inlet$	inlet
max	maximum
o	oxygen
s	solvent

Greek Symbols

δ	adjusted constant for pulse valve equation
ΔH	heat of polymerization
ΔP_{fr}	pressure drop due to friction per unit of reactor length
ΔP_{pvi}	pressure drop due to pulse between location i-1 and i
γ	adjusted constant for pulse valve equation
$\lambda_{m,n}$	m^{th}, n^{th} moment for radical chain length distribution
ρ	density of the reacting mixture
$\mu_{m,n}$	m^{th}, n^{th} moment for polymer chain length distribution

REFERENCES

1. A. Brandolin, M. H. Lacunza, P. E. Ugrin, and N. J. Capiati, *Polym. Reaction Eng.*, **4**, 296 (1996).
2. R. C. M. Zabisky, W.-M. Chan, P. E. Gloor, and A. E. Hamielec, *Polymer*, **33**, 2243 (1992).

3. S. K. Gupta, A. Kumar, and M. V. G. Krishnamurthy, *Polym. Eng. Sci.*, **25**, 37 (1985).
4. P. Lorenzini, M. Pons, and J. Villermaux, *Chem. Eng. Sci*, **47**, 3981 (1992).
5. C. Kiparissides, G. Verros, G. Kalfas, M. Koutoudi, and C. Kantzia, *Chem. Eng. Comm.*, **121**, 193 (1993).
6. C. H. Chen, J. G. Vermeychuk, S. A. Howell, and P. Ehlrich, *AIChE J.*, **22**, 463 (1976).
7. S. Agrawal and C. D. Han, *AIChE J.*, **21**, 449 (1975).
8. K. H. Lee and J. P. Marano, Jr., in *Polymerization Reactors and Processes*, J. N. Henderson and T. C. Bouton, eds., *ACS Symposium Series*, **104**, American Chemical Society: Washington, D.C., 221 (1979).
9. H. Mavridis and C. Kiparissides, *Polym. Proc. Eng.*, **3**, 263 (1985).
10. K. H. Goto, S. Yamamoto, S. Furui, and M. Sugimo *Appl. Polym. Sci.: Appl. Polym. Symp.*, **36**, 21 (1981)
11. G. Donati, M. Marini, L. Marziano, C. Mazzaferr Spampinato, and E. Langianni, in *Chemical Rea Engineering*, J. Wei and C. Georgakis, eds., *ACS Sy sium Series*, **196**, American Chemical Society: W ington, D.C., 579 (1981).
12. P. P Shirodkar and G. O. Tsien, *Chem. Eng. Sci.*, 1031 (1986).
13. A. Brandolin, N. J. Capiati, J. N. Farber, and E. M. lés, *Ind. Eng. Chem. Res.*, **27**, 784 (1988).
14. J. Villermaux, M. Pons, and L. Blavier, *Inst. Ch Engng. Symp. Ser.*, **87**, 553 (1984).
15. M. H. Lacunza, P. E. Ugrin, N. J. Capiati, and A. Br dolin, *Polym. Eng. Sci.*, **38**, 992 (1998).